CONTROLLING TRIPARTITE ENTANGLEMENT BY EXTERNAL PULSING

J. A. Roversi
Instituto de Fisica "Gleb Wataghin"
Universidade Estadual de Campinas
Unicamp, Campinas, São Paulo, Brazil
roversi@ifi.unicamp.br

J. C. Gonzalez-Henao
Instituto de Fisica "Gleb Wataghin"
Universidade Estadual de Campinas
Unicamp, Campinas, São Paulo, Brazil
juliocg@ifi.unicamp.br

E. Pugliese
Istituto Nazionale di Ottica
Consiglio Nazionale delle Ricerche
Largo E. Fermi 6, 50125 Firenze, Italy
eugenio.pugliese@ino.it

R. Meucci
Istituto Nazionale di Ottica
Consiglio Nazionale delle Ricerche
Largo E. Fermi 6, 50125 Firenze, Italy
riccardo.meucci@ino.it

S. Euzzor
Istituto Nazionale di Ottica
Consiglio Nazionale delle Ricerche
Largo E. Fermi 6, 50125 Firenze, Italy
stefano.euzzor@ino.it

F. T. Arecchi
Istituto Nazionale di Ottica
Consiglio Nazionale delle Ricerche
Largo E.Fermi 6, 50125 Firenze, Italy
tito.arecchi@ino.it

Abstract
We exploit the relationship between classical instability and entanglement to control the creation of entangled states in an open system of three coupled quantum parametric oscillators at high temperature. Introducing a suitable pulsed perturbation in the classical system we are able to control the transition from stable to unstable behaviour. Entanglement arises in the same parameter regions where the classical system is unstable displaying features different from the case of two coupled oscillators. Entangled states are particularly sensitive to negative pulses and to the size of the duty cycle.

Key words
Entanglement, quantum control, dynamic instability

1 Introduction

In the last decades, the peculiar features of quantum mechanics have been exploited in multiparty systems to introduce promising information methodologies. Although superposition effects in composite systems are well known in classical physics, a new quantum-mechanical effect arises when a tensor product structure for the space of states is considered,namely, quantum states can be entangled. Based on this feature, it has been realized that entangled states allow new practical applications, ranging from quantum computation [Barenco, 1996 ; Vedral and Plenio, 1998] and secure cryptographic schemes [Bennett and Brassard, 1984; Ekert, 1991] to improved optical frequency standards [Bollinger, Itano, Wineland, Heinzen, 1996; Huelga, Macchiavello, Pellizzari, Ekert, Plenio and Cirac, 1997]. In view of this, many efforts, both at the theoretical and experimental level, have been made to better understand and control such a quantum property. Particular interest has been devoted to the interaction with a hot environment which determines in general the disappearance of quantum behaviour. Several schemes have been proposed to overcome or, at least, reduce the influence of temperature in the loss of coherence. Duan and Guo [Duan and Guo, 1997] proposed to pair each qubit with an ancilla qubit and to encode the states of the system into states of qubit pairs. On the same line Gonzalez-Henao and Roversi [Gonzalez-Henao and Roversi, 2015] have proposed a third qubit to protect entanglement in a two qubit system at high temperature regime. In this communication we use an external pulse to control the dynamic instabilities in a system of three coupled oscillators. The pulse drives the quantum system towards or away from entangled states. This feature allows to maintain the entanglement state for a long time. In our view, this method may open a way for manipulating quantum features at high temperature regimes.

2 Theory and results

Here we consider a system of three coupled quantum parametric oscillators in equilibrium with a common heat bath at a temperature different from zero. The Hamiltonian of the system for N oscillators is:

$$H_T = H_S + H_{SR} \tag{1}$$

$$H_S = \frac{1}{2}\sum_{i=1}^{N}\left[\frac{P_i^2}{m_0} + m_0\omega^2(t)X_i^2\right] + \sum_{i>j=1}^{N} c(t)X_iX_j \tag{2}$$

$$H_{SR} = \sum_{k=1}^{\infty}\left[\frac{p_k^2}{2m_k} + \frac{m_k\omega_k^2x_k^2}{2} - \sqrt{2}c_kx_k\left(\sum_{i=1}^{N}X_i\right) + \frac{c_k^2}{2m_k\omega_k^2}\left(\sum_{i=1}^{N}X_i\right)^2\right] \tag{3}$$

The total Hamiltonian H_T is given by H_S that represents a system of N oscillators and their interactions and H_{SR} representing the interaction between oscillators and thermal reservoir. $\omega(t)$ is the angular frequency and $\{X_i, P_i\}$ are the position and momentum operators for the oscillators; ω_k and $\{x_k, p_k\}$ are the corresponding quantities for the environment oscillators. Each one of these oscillators is coupled to the others by the function $c(t)$ and connected to the environment through the constants c_k.

In order to diagonalize the Hamiltonian H_T we use the transformation $[X] = R.[X']$ and $[P] = R.[P']$ based on the orthogonal matrix R defined in [Gonzalez-Henao, Pugliese, Euzzor, Meucci, Roversi and Arecchi, 2017, supplementary information]:

$$R = \begin{pmatrix} \frac{1}{\sqrt{3}} & 0 & -\sqrt{\frac{2}{3}} \\ \frac{1}{\sqrt{3}} & \frac{1}{\sqrt{2}} & \frac{1}{\sqrt{6}} \\ \frac{1}{\sqrt{3}} & -\frac{1}{\sqrt{2}} & \frac{1}{\sqrt{6}} \end{pmatrix} \tag{4}$$

that transforms H_T, for the case of three oscillators, into the following form:

$$H_T = H_1' + H_2' + H_3' \tag{5}$$

$$H_1' = \frac{1}{2}\left[\Omega_+^2(t)X_1'^2 + P_1'^2\right] + \sum_{k=1}^{\infty}\left(\frac{p_k^2}{2} + \frac{\omega_k^2x_k^2}{2} - \sqrt{2}c_kx_kX_1' + \frac{c_k^2}{2\omega_k^2}X_1'^2\right) \tag{6}$$

$$H_2' = \frac{1}{2}\left[\Omega_-^2(t)X_2'^2 + P_2'^2\right] \tag{7}$$

$$H_3' = \frac{1}{2}\left[\Omega_-^2(t)X_3'^2 + P_3'^2\right] \tag{8}$$

where $\Omega_+^2(t) = [\omega(t)^2 + 2c(t)/m_0]/\omega_0^2$ and $\Omega_-^2(t) = [\omega(t)^2 - c(t)/m_0]/\omega_0^2$ are the effective frequencies of the second and third parametric oscillator.

The main difference between the case with two and three oscillators is the presence of the additional decoupled parametric oscillator of coordinates $(X_3'^2, P_3'^2)$. The case of two parametric oscillators was studied in [Gonzalez-Henao, Pugliese, Euzzor, Abdalah, Meucci and Roversi, 2015]. The effective frequencies $\Omega_\pm^2(t)$ of the systems with $N = 2$ and $N = 3$, depend on the functions $\omega(t)$ and $c(t)$. We specialized the discussion to the case $c(t) = cm_0\omega_o^2$ and $\omega(t)^2 = \omega_o^2[1 + A(1 + mf(t))cos(\omega_d t)]$ where ω_d is an external driving pulsation. The function $f(t)$ regulates the amplitude of the function $\Omega_\pm^2(t)$, as shown in Fig.1. A dimensionless pulsation can be introduced as $\Omega_-^2 = [\omega(t)^2 - c(t)/m_0]/\omega_0^2 = \omega(t)^2/\omega_o^2 - c = \omega_r^2 + A[1 + mf(t)]cos(\omega_d t)$, with $\omega_r^2 = 1 - c$. The periodic function $f(t)$ is defined as:

$$f(t) = \begin{cases} 0 & \text{if } 0 < t < a \\ 1 & \text{if } a < t < b + a \end{cases} \quad \text{with } a + b = 2\pi/\omega_d.$$

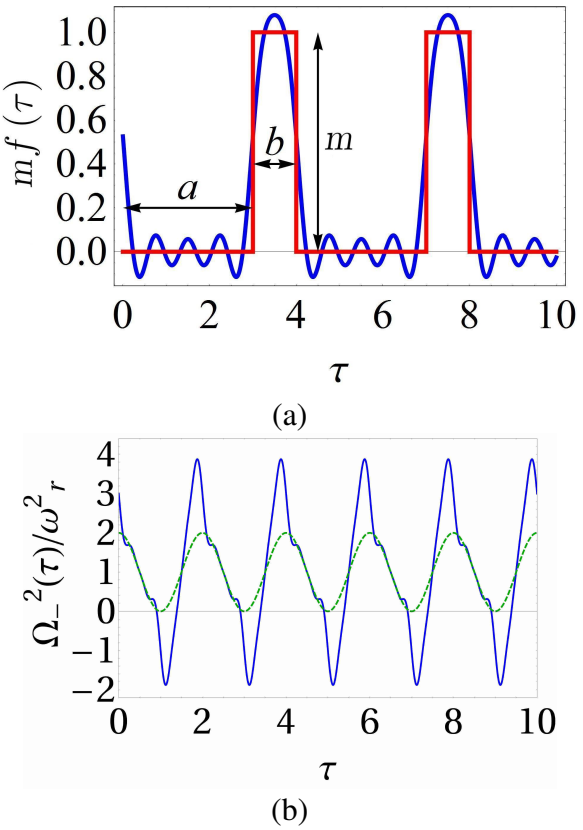

Figure 1. (a) Schematic representation of the external perturbation $mf(\tau)$: the blue curve is the result of superposition of the first five Fourier harmonics ($a = 1$ and $b = 1$); the red step function is the experimental stimulus introduced into the Mathieu's oscillator. (b)Schematic representation of the $\Omega(t)_-^2/\omega_r^2$ as a function of the time $\tau = \omega_0 t$ with $m = 0$ (green line) and $m = 2$ (blue line)

Considering that the introduced coordinate transforma-

tion $X \rightarrow X'$ is orthonormal, it can be easily shown that the operators X' and X satisfy the same commutation rules. This also implies that the solutions can be found independently. As initial condition we consider coherent states $\hat{\rho}(0) = |\Psi\rangle\langle\Psi|$ where $|\Psi\rangle = |\alpha_1\alpha_2\alpha_3\rangle$. In the new coordinate system these states do not change in form since they remain coherent states. The only change is the coefficient α which obeys the same transformation of the coordinate system. The coherent character of the initial Gaussian state is preserved by the orthonormal transformation originated from R and it is maintained during the time evolution due to the bilinear character of the Hamiltonian (6). This implies that every quantum correlation can be obtained from the Covariance Matrix (CM) whose elements are given by

$$\sigma_{\mathcal{R}_i\mathcal{R}_j} = \frac{1}{2}\langle \mathcal{R}_i\mathcal{R}_j + \mathcal{R}_j\mathcal{R}_i\rangle - \langle \mathcal{R}_i\rangle\langle \mathcal{R}_j\rangle \quad (9)$$

with $[\mathcal{R}] = (X_1, P_1, X_2, P_2, X_3, P_3)$. The CM elements are more easily obtained by first calculating them in the prime coordinates $(X_1', P_1', X_2', P_2', X_3', P_3')$ and then using the inverse transformation to determine them in the initial coordinates $(X_1, P_1, X_2, P_2, X_3, P_3)$.

To calculate the CM elements for the Hamiltonians (7) and (8)) we have used the Heisenberg representation, whereas to obtain the CM elements of the Hamiltonian (6) we have used the Feynman's path integral formulation [Feynman and Hibbs, 1965], [Caldeira and Leggett,1983] as we have already done for two oscillators [Gonzalez-Henao, Pugliese, Euzzor, Abdalah, Meucci and Roversi, 2015].

Roque et al. [Roque and Roversi, 2012] and Gonzalez-Henao et al. [Gonzalez-Henao, Pugliese, Euzzor, Abdalah, Meucci and Roversi, 2015] showed that the onset of the quantum entanglement is strongly tight to the presence of diverging solutions of the CM element equations of the operators X' and P'. In particular, only the CM elements of the oscillator Ω_- are crucial in this analysis. Their amplitude $\mathbb{X}_-$ evolves in time according to the following differential equation,

$$\ddot{\mathbb{X}}_-(t) + \Omega_-^2(t)\,\mathbb{X}_-(t) = 0. \quad (10)$$

In terms of first order differential equations the system dynamics is ruled by :

$$\begin{cases} \dot{x} = y \\ \dot{y} = -\{\omega_r^2 + A\,[1 + mf(\tau)]\,cos(\tilde{\omega}_d\tau)\}x \end{cases} \quad (11)$$

where we assumed $\tilde{\omega}_d = \omega_d/\omega_o$ and $\tau = t\omega_o$, with ω_o related to the ground state energy of quantum oscillators. The term $m \cdot f(\tau)$ represents the analytic form of the external stimulus consisting of a pulse train with adjustable amplitude and duty cycle (see blue curve in Fig.1(a)). The factor m plays a crucial role in the transition to entangled states and, at variance with the case recently explored in [Gonzalez-Henao, Pugliese, Euzzor, Meucci, Roversi and Arecchi, 2017], negative values of m are more effective as we will show.

Experimental — The experimental tests were performed on an electronic analog circuit obeying to Eq. 11 where the function $f(t)$ is a square wave function. Adjusting the parameters m, A and $\tilde{b} = b/(a+b)$ we were able to determine the boundaries between the stable and the unstable regions. In Fig.2(a) the red dots indicate these boundaries for $m = 0$. The stability map in the plane $\tilde{b}$ - m for $\tilde{\omega}_d/\omega_r = 2.06$ is shown in Fig.2 (b). From a mathematical point of view, the system is stable in the regions where the Floquet coefficient is zero ($\mu = 0$) and it is unstable in the regions where $\mu > 0$, respectively. The blue color in Fig.2 (b) indicates the stable region (see side color bar in Fig.2(b) for Floquet coefficient μ). The experimental points were overlaid on the numerical simulations.

Quantum approach — As the system evolves as a Gaussian state we can consider the positive partial transposition theorem (PPT) [Peres, 1996; Simon, 2000] as a criterion for quantum entanglement. Here we extend the description of the bipartite entanglement to the system of three parametric oscillators. This can be done by considering subdivisions of the global system into the subsystems formed by one oscillator and the subsystem composed by the other two remaining oscillators. As the Hamiltonian in Eq. 1 is invariant under oscillator exchanges we can show that bipartite entanglement is invariant with respect to the chosen subdivision, whether it is $1|23$, $2|13$ or $3|12$. This is a manifestation of the fact that CM is fully symmetric. Thus to quantify the bipartite entanglement of the three oscillators system (between the oscillator 1 and the oscillators 2 and 3) we use the bipartite Logarithmic Negativity given by

$$E_N^{1|23} = \begin{cases} 0 & if\ \tilde{n}_- \geq 1 \\ -\log\tilde{n}_- & if\ \tilde{n}_- < 1 \end{cases} \quad (12)$$

where $\tilde{n}_-$ is a symplectic eigenvalue of the CM transpose (only one of the 6 symplectic eigenvalues of the σ transpose can be negative) of the system with three oscillators [Adesso, Serafini, and Illuminati, 2004].

Results — In all calculations we used the following values $A = 0.215$, $\tilde{\omega}_d/\omega_r = 2.06$, $c = 0.0591$, temperature of the reservoir $\tilde{T} = K_BT/\hbar\omega_0 = 100$ and dissipation rate $\gamma = 0.01\omega_0$, for three values of m, (i.e, $m = -0.5$, $m = -1.5$, $m = -2.5$). The initial condition of the system with three oscillators is the coherent state $|\Psi\rangle = |\alpha_1\alpha_2\alpha_3\rangle$ $\alpha_1 = -\alpha\left(\sqrt{2}-1\right)/\sqrt{3}$, $\alpha_2 = \alpha\left(3\sqrt{2}+2\sqrt{3}+\sqrt{6}\right)/6$ and $\alpha_3 = \alpha\left(-3\sqrt{2}+2\sqrt{3}+\sqrt{6}\right)/6$. This state in the coordinates '$\prime$' is $|\Psi\rangle = |\alpha\alpha\alpha\rangle$ with $\alpha = 1/\sqrt{2}$. For

comparison we present results for the case of two oscillators with the initial condition being a coherent state $|\Psi\rangle = |\sqrt{2}\alpha 0\rangle$ and in the coordinates 'r' $|\Psi\rangle = |\alpha\alpha\rangle$. In Fig.2 (c) we report, for $m = -0.5$, the logarithmic negativity $E_N^{1|23}$ against the dimensionless time τ, for different values of the duty cycle $\tilde{b}$. For values of $\tilde{b}$ for which $\mu = 0$ (see Fig.2 (b)) the system does not present entanglement. Otherwise, only for $\tilde{b}$ closed to 1, where $\mu = 0$ and after a certain threshold time the system presents entanglement. Once the system has acquired entanglement, it approximately grows linearly with small superimposed oscillations. Fig.2 (c), (d) and (e) shows the bipartite logarithmic negativity $E_N^{1|23}$ for $m = -0.5$, $m = -1.5$ and $m = -2.5$, respectively. As it can be seen $\tilde{b}$ is of great importance for the control of entanglement. This is shown in the Fig.2 (c) where for all values of $\tilde{b}$ there is entanglement and in Fig.2 (d) where a narrow region of $\tilde{b}$ allows entanglement. The pulse intensity m is the most relevant parameter in the definition of dynamic instabilities. It causes the system to range from full entanglement to any value of the pulse width, $\tilde{b}$, or even to a negligible amount of entanglement. Fig.2 (c) and in Fig.2 (d) represent the signature of this behavior. This strong correlation between instability and entanglement supported by parametric pathways (intensity and width of the external pulse) allows us to sustain entanglement for long periods of time and at high temperatures. This brings us a support in the search for more robust systems against decoherences and in the processing of quantum information.

We have also observed that for the same values of $\tilde{b}$ and $\mu > 0$ where entanglement is detected for three oscillators, a similar behaviour emerges for two oscillators with the difference that the function $E_N^{1|23}(\tau) < E_N(\tau)$. This reduction of entanglement, due to the third oscillator, is consistent with the monogamy inequality conjectured by Coffman, Kundu and Wootters [Coffman, Kundu and Wootters, 2000] and extended by Osborne and Verstraete [Osborne and Verstraete, 2006]. Figure 3 (a) reports the initial entanglement time against $\tilde{b}$ for two (blue curve) and three (red curve) oscillators showing that entanglement occurs first in latter case, but the entanglement $E_N^{1|23}$ is less than that for two oscillators. This is due to the fact that the system with three oscillators has more degrees of freedom, which create faster entanglement.
In Fig.3 (b) the mean entanglement rate $E_N^{1|23}$ and the real part of the Floquet coefficient μ corresponding to Fig.2 (d) and Fig.2 (c) are plotted. In these figures we can see that the behavior of ζ and μ is similar, although in the region $0.55 < \tilde{b} < 1.00$ a change in the concavity of μ as function of $\tilde{b}$ arises. In the inset of Fig.3 (b) a plot of ζ as a function of μ is reported. In the interval $0.00 < \tilde{b} < 0.06$ the behavior of ζ is approximately linear, whereas in the interval $0.55 < \tilde{b} < 1.00$ ζ it shows a discontinuous behavior due to a change in the concavity of μ versus $\tilde{b}$.
Figure 4 (a) shows the bipartite logarithmic nega-

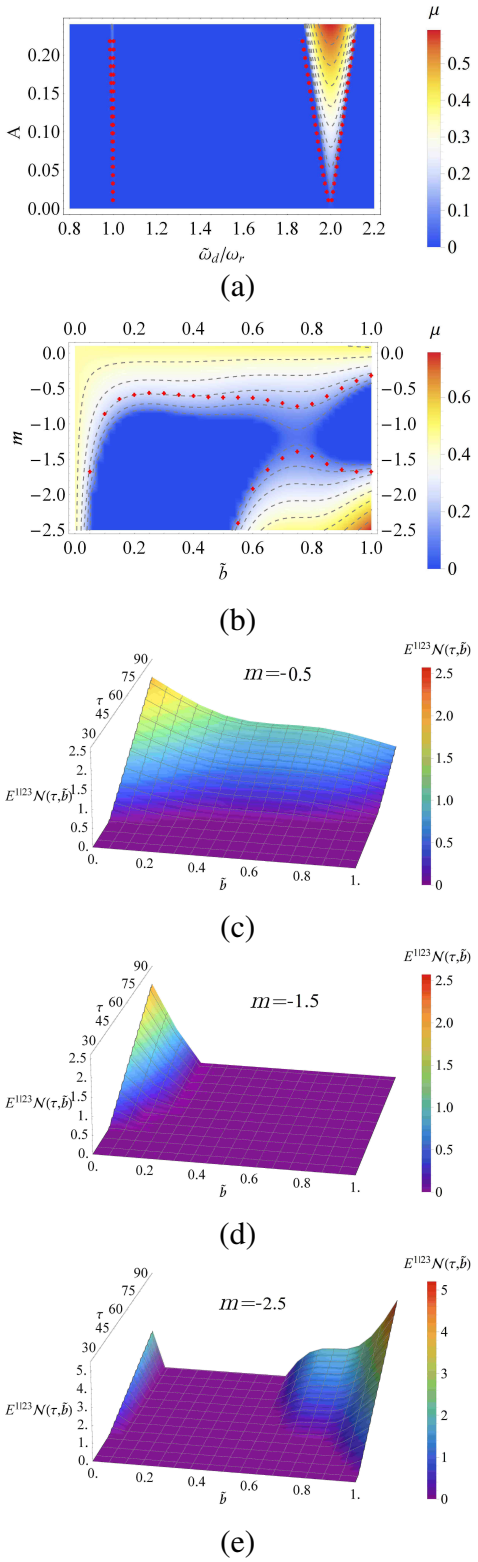

Figure 2. (a) Stability map A vs $\tilde{\omega}_d/\omega_r$ of the dynamical system (10) for $m = 0$; (b) Stability map m vs $\tilde{b}$ for the (10), assuming $\tilde{\omega}_d/\omega_r = 2.06$ and $A = 0.215$. The colorbars are associated with the Floquet coefficient μ. (c), (d) and (e) Logarithmic negativity $E_N^{1|23}$ vs τ, for $N = 3$ oscillators and $m = -0.5$, $m = -1.5$ and $m = -2.5$, respectively ($\tilde{\omega}_d/\omega_r = 2.06$ and $A = 0.215$.

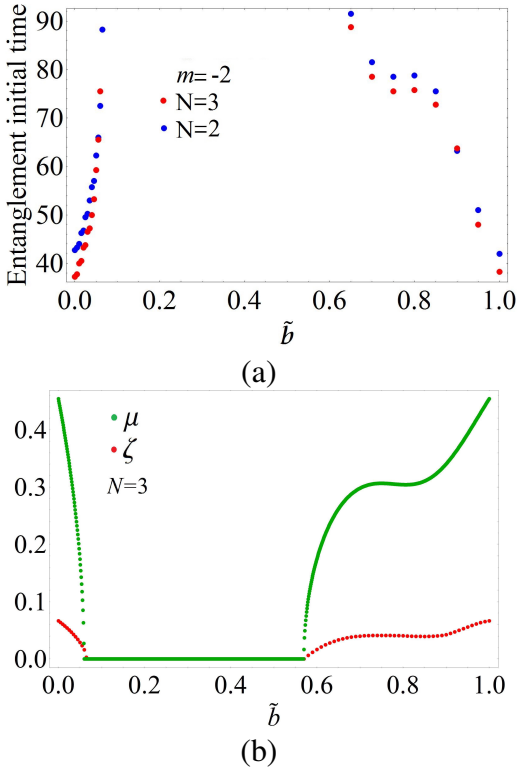

Figure 3. (a) Plots of the initial entanglement time for two (blue dots) and three (red dots) oscillators respectively. (b) Real part of the Floquet coefficient μ and average rate ζ of bipartite entanglement $E_N^{1|23}$ as a function of $\tilde{b}$ with the same parameters as in (a). Parameter values: $\tilde{\omega}_d/\omega_r = 2.0$, $A = 0.215$ and $m = -2.0$.

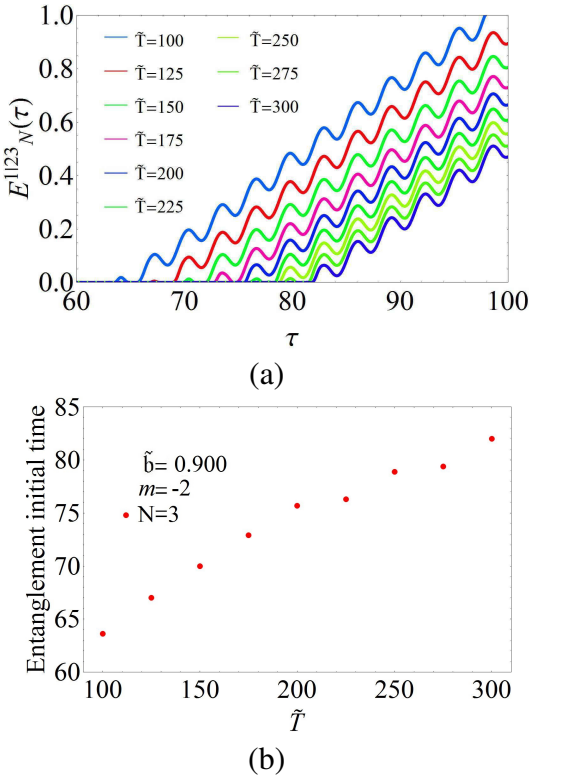

Figure 4. (a) Plots of the bipartite entanglement as a function of time τ for the system with three oscillators for different values of temperature $\tilde{T}$. (b) Entanglement initial time function of the temperature $\tilde{T}$ to the same parameters as in (a). For the two plots we have used $\tilde{\omega}_d/\omega_r = 2.0$, $A = 0.215$, $\tilde{b} = 0.900$ and $m = -2.0$

tivity $E_N^{1|23}$ for three oscillators as function of τ for different temperature values. As it can be seen an increase of temperature does not change the behavior of the entanglement. Figure 4 (b) shows the initial entanglement time against $\tilde{T}$, showing an almost linear behavior between these two quantities. As it can be seen from Fig.4, also in the case of tripartite system, the entanglement persists even at high temperatures.

3 Conclusions

In this work we considered the bipartite quantum entanglement for a system of three oscillators in contact with a thermal reservoir at high temperature. The analysis of the classical counterpart explored on a single parametric oscillator is of crucial importance because it allows to know the regions where entanglement will be originated. Peculiar differences emerge when negative perturbations are used. Minor perturbations are required to enter in a entanglement region . For particular m values the transition is controlled by the other parameter $\tilde{b}$ in two distinct regions. This strong correlation between dynamic instability and entanglement supported by parametric pathways encourages us to continue searching for more robust systems in the case of decoherence and quantum information processing.

References

A. Barenco, Contemp. Phys. **37**, 375 (1996); V. Vedral and M.B. Plenio, Prog. Quantum Electron. **22**, 1 (1998).

C.H. Bennett and G. Brassard, in Proceedings of the IEEE International Conference on Computers, Systems and Signal Processing, Bangalore, India IEEE, New York, p. 175, (1984); A. K. Ekert, Phys. Rev. Lett. **67**, 661 (1991).

J. J. Bollinger, W. M. Itano, D. J. Wineland, and D. J. Heinzen, Phys. Rev. A 54, R4649 (1996); S. F. Huelga, C. Macchiavello, T. Pellizzari, A. K. Ekert, M. B. Plenio, and J. I. Cirac, Phys. Rev. Lett. 79, 3865 (1997).

L.M. Duan and G.C. Guo, Preserving Coherence in Quantum Computation by Pairing Quantum Bits, *Phys. Rev. Lett.* **79**, 1953 (1997).

J.C. Gonzalez-Henao and J.A. Roversi, Decrease of the decay rate of the entanglement of a system of two entangled qubits by increasing the temperature of the thermal bath, *Quantum Information Processing* **14**, 1377 (2015).

J.C. Gonzalez-Henao, E. Pugliese, S. Euzzor, S.F. Abdalah, R. Meucci, and J.A. Roversi, Generation of entanglement in quantum parametric oscillators using phase control, *Sci. Rep.* **5**, 13152 (2015).

T.F. Roque and J.A. Roversi, The role of instabilities in

the survival of the quantum correlations, *Phys. Rev. A* **41**, 726 (2012).

R.P. Feynman and A.R. Hibbs, *Quantum Mechanics and Path Integrals* (McGraw-Hills Companies, New York, 1965).

A.O. Caldeira and A.J. Leggett, Path integral approach to quantum Brownian motion, *Physica A* **121**, 587 (1983).

J.C. Gonzalez-Henao, E. Pugliese, S. Euzzor, R. Meucci, J.A. Roversi, and F.T. Arecchi, Control of entanglement dynamics in a system of three coupled quantum oscillators, *Sci. Rep.* **7** 9957, (2017).

A. Peres, Separability criterion for density matrices, *Phys. Rev. Lett.* **77**, 1413 (1996).

R. Simon, Peres-Horodecki criterion for continuous variable systems, *Phys. Rev. Lett.* **84**, 2726 (2000).

G. Adesso, A. Serafini, and F. Illuminati, Quantification and scaling of multipartite entanglement in continuous variable systems, *Phys. Rev. Lett.* **93**, 220504 (2004).

V. Coffman, J. Kundu, and W.K. Wootters, Distributed entanglement, *Phys. Rev. A* **61**, 052306 (2000).

T.J. Osborne and F. Verstraete, General monogamy inequality for bipartite qubit entanglement, *Phys. Rev. Lett.* **96**, 220503 (2006).